

Factors Affecting Solvent Retention due to Gel Formation during Dissolution-Based
Plastic Recycling

By
Hedam Kim

A thesis submitted in partial fulfillment of
The requirements for the degree of

Master of Science
(Chemical and Biological Engineering)

at the
UNIVERSITY OF WISCONSIN-MADISON
2025

I certify I have read this report and that, in my opinion, it is fully adequate in scope and quality as a report for the degree of Master of Science.

Professor George Huber (advisor)

Abstract

Dissolution-based recycling provides a way to recover polymers from mixed plastic waste, but a large amount of energy is required to remove residual solvent after precipitation.^{1,2} In this study, we measured the solvent retention of 34 polymer-solvent systems consisting of eight polymers and nine solvents to understand what controls solvent retention. Solvent retention ranged from 20.16 to 91.65%, showing that different polymer-solvent pairs behave very differently.

Cooling rate, precipitation method, and filtration time did not significantly change solvent retention. Instead, solvent volatility, polymer molecular weight, and polymer-solvent affinity were the main variables that have influence on the amount of solvent remaining in polymer-solvent gels. Volatile solvents such as xylene consistently exhibits low solvent retention, while solvents with lower vapor pressure resulted in higher retention.³

A support vector regression model was developed to predict the solvent retention using multiple features. A leave-one-out technique was used to quantify the contribution of each feature. Initially, a six-feature model was developed and further feature reduction to five-, and four-feature models was performed based on leave-one-out results. Among them, five-feature model shows the highest R^2 of 0.78 and the lowest Akaike information criterion and Bayesian information criterion values, suggesting that five-feature without the Flory-Huggins interaction parameter is the ideal for predicting the solvent retention. Vapor pressure was the most important variable, followed by polymer molecular weight.

This work can contribute to framework for solvent selection and for predicting solvent retention in more complex feed stocks such as multilayer waste. This approach may also guide more efficient STRAPTM process design.

Acknowledgement

I would like to express my deepest gratitude to my advisor, Professor George Huber for giving me the opportunity to conduct research in his group. I greatly respect his passion and dedication to science. I have learned much about the scientific method, how to bridge between science and industry, and how to communicate scientific findings effectively. I am sincerely grateful for his time, efforts, and mentoring, and I will continue to carry the lessons I have learned under his guidance.

I would also like to thank my committee members, Professor Reid Van Lehn, Professor Whitney Loo, and Professor Styliana Avraamidou, for their continued support and investment in me. I am especially grateful to Professor Reid Van Lehn for his insightful scientific discussions and for helping me shape the conceptual framework and discussion of my manuscript. I also appreciate the valuable advice from my committee during my preliminary exam, which helped me identify how to move my research forward.

I would like to extend my thanks to the CBE administrative team, especially Kate Fanis, who has guided me through every administrative challenge and has always been the first person I turn to when I have rough days in Madison.

I am also thankful to the members of the Huber group and collaborators for scientific discussion, advice and emotional support. I would like to acknowledge Lily Callen, Tushar, Hoya Ihara, Javier Chavarrio, Shriya Sharma, Charles Granger, Seonyeong Kim, Dr. Euncheol Na, Dr. Leoncio Santiago, Dr. Jiayang Wu for their help and encouragement. I am grateful to Ali Altamimi for collaborating with me on solvent retention work, providing the predicted solubility data and putting input on the prediction

model together. I would like to thank to the members of the Loo group, especially Marissa Gallmeyer, Jenny Wu, and Jingchao Qin for assistance with WAXS measurements and discussion about the results. In addition, I appreciate to Meng-Lin Tsai and Parth Brahmhatt for discussions on modeling. I would not have been able to complete my degree without them.

I am deeply grateful to my friends and family, who have always believed in my potential and supported me unconditionally. Special thanks to Seonyeong Kim (again), Jukbin Kim, Geunryeol Baek, Hochang Song, Michelle Choi, Somin Chae, and Kyungjin Sohn, for keeping me afloat my frustrating days in Madison. I am very lucky to build the friendships with them and have them in my life. Thank you to my dog, Merry for always cheering me up and keeping me going during difficult moments.

Lastly, I want to express my heartfelt gratitude to my parents for endless support even during uncertain times. As the first in my family to attend college and pursue graduate studies abroad, their encouragement has meant the world to me. They have supported my journey every step of the way, allowing me to complete my degree at the University of Wisconsin- Madison.

List of Tables

| | |
|---|----|
| Table 1. Hyperparameters of Model 1, 2, and 3..... | 13 |
| Table 2. Solvent retention when anti-solvent is added..... | 17 |
| Table 3. Solvent retention of PP and decanol with 5 wt% with different filtration time. | 21 |
| Table 4. Solvent retention in polymer-solvent gels with six variables including polymer-to-solvent ration (r), polymer molecular weights (M_w), solvent vapor pressure (P_{vap}), solvent Hansen solubility parameter (δ_T), predicted solubility (S_{pred}), and Flory-Huggins interaction parameter (χ). | 23 |
| Table 5. Models with six, five, and four features and their fitness and complexity. | 32 |

List of Figures

| | |
|---|----|
| Figure 1. Experimental procedure for STRAP™. Polymer is dissolved in hot solvent, precipitated by cooling, vacuum-filtered, and finally dried in an oven to remove residual solvent. | 8 |
| Figure 2. Schematic illustration of a jacketed vessel with two necks connected to a chiller. | 9 |
| Figure 3. Conceptual schematic of polymer-solvent system during STRAP™. Blue dots and gray lines indicate solvent molecules and polymer chains. | 15 |
| Figure 4. (a) Temperature profiles of hot polymer solution, cooled isothermally at different bath temperatures. The shaded region was used to determine the cooling rate. (b) Solvent retention and crystallinity as functions of the cooling rate. | 16 |
| Figure 5. Images of 2 g of polymers (LDPE, PP-L, and PP-H) dissolved in 150 g of xylene precipitated at different temperatures in the jacketed vessel after 1 hr. | 19 |
| Figure 6. DSC curves (2 nd heating cycling) for recovered PP and LDPE. | 20 |
| Figure 7. Box and scatter plot of measured solvent retention. The box shows the interquartile range with the median line. The “x” marks the average and two whiskers span the minimum and maximum values. | 26 |
| Figure 8. Spearman’s rank correlation coefficient between each variable and solvent retention. | 27 |
| Figure 9. Tested R ² of different models with six, five, and four features. | 29 |
| Figure 10. Parity plot of (a) six-, (b) five-, and (c) four-feature models. | 30 |
| Figure 11. Leave-one-out analysis for (a) six-, (b) five-, and (c) four-feature models. | 31 |

Table of Contents

| | |
|---|-----|
| Abstract..... | v |
| Acknowledgement | vii |
| List of Tables | ix |
| List of Figures | x |
| 1. Introduction..... | 1 |
| 2. Background..... | 4 |
| 2.1 Polymer-solvent thermodynamics..... | 4 |
| 2.2 Polymer precipitation and gel formation..... | 5 |
| 2.3 Diffusion in polymer-solvent gels..... | 6 |
| 2.4 Motivation for this work | 6 |
| 3. Experimental methods | 7 |
| 3.1 Materials..... | 7 |
| 3.2 STRAP TM Experimental Procedure..... | 7 |
| 3.3 Cooling rate-controlled precipitation | 9 |
| 3.4 Wide-Angle X-ray Scattering (WAXS) | 9 |
| 3.5 Differential Scanning Calorimetry (DSC)..... | 10 |
| 3.6 Determination of variables | 10 |
| 3.7 SVR model | 12 |
| 3.8 Model selection | 13 |
| 4. Results and discussion | 15 |
| 4.1 Conceptual overview of STRAP TM | 15 |
| 4.2 Effect of cooling rate on crystallinity and solvent retention | 16 |
| 4.3 Different precipitation methods | 17 |
| 4.4 Selective precipitation of PP and PE..... | 18 |
| 4.5 Effect of filtration time on solvent retention..... | 21 |
| 4.6 Solvent retention in different polymer-solvent gels..... | 22 |
| 4.7 SVR model and model selection..... | 28 |
| 5. Conclusions..... | 33 |
| 6. Future work..... | 34 |
| 7. References..... | 35 |

1. Introduction

Plastics are among the most widely produced materials because of their low cost, chemical versatility, and desirable mechanical properties.^{4,5} Global plastic production has reached approximately 380 million tons per year, and the cumulative amount of plastics produced is projected to exceed 30 billions tons by 2050.^{6,7} This continued growth has highlighted long-standing concerns related to plastic waste management and environmental persistence. Mechanical recycling often suffers from polymer degradation, contamination, and material property loss, which restricts its applicability to multilayer or composites films that are widely used in food packaging and consumer products.⁸

Solvent-Targeted Recovery and Precipitation (STRAPTM), first proposed by Walker et al., offers an alternative approach by using polymer-solvent solubility differences to selectively recover polymers from complex plastic wastes.⁹ STRAPTM consists of four main steps: selective polymer dissolution, separation of undissolved fractions, precipitation to form a polymer-solvent gel, and vacuum filtration followed by drying.¹ Prior studies have demonstrated that the process can remove contaminant, clean dissolved polymers, and recover resins with minimal degradation, even after repeated recycling cycles.¹⁰⁻¹² STRAPTM does not rely on high temperatures or reactive chemistries, and it has been used to recover a broad range of polymers from multilayer structures and complex feedstocks.^{10,12-14}

Recent work has shown that STRAPTM can sequentially recover up to ten different polymers from post-industrial mixed plastic waste by using computed solubility windows and step-by-step dissolution.¹⁰ In addition, STRAPTM can remove pigments, ink, and other additives embedded within polymer layers and generate color-free and

contaminant-free resins.^{11,12} This deep cleaning capability is one of the advantages over mechanical recycling, which often retained these contaminants in the recycled plastic.

STRAPTM has additionally demonstrated the different methods of precipitation. This should include the Kevin's anti-solvent and temperature-controlled work.² Reducing anti-solvent use is more beneficial because there is no further distillation process required to recycle the solvent.

Beyond packaging films, STRAPTM has been applied to other waste streams such as disposable biomanufacturing plastics and facial masks. Tushar et al. recently recovered polyethylene and ethylene vinyl alcohol from single-use biocontainer systems provided by Cytiva, and the quality of resulting films are similar to the virgin LDPE cast film in color, haze, and transmittance.¹⁵ Also, Yu et al. used STRAPTM technology to extract polypropylene from disposable face masks, showing 90 wt% recovery.¹⁴ These studies reveal that STRAPTM can meet material purity and performance requirements for remanufacturing, demonstrating potential for integration into closed-loop recycling systems.

Although extensive efforts have focused on solvent screening, dissolution design, precipitation strategies, and feedstock-specific studies, the behavior of solvent entrapped in a polymer matrix remains poorly understood.¹⁶⁻¹⁸ During STRAPTM, precipitation produces slurry that contains both freely draining solvent and solvent tightly held within polymer domains. Mechanical vacuum filtration removes only the easily drained portion approximately 30% of total solvents, leaving a significant amount of solvent entrapped. This remaining solvent must be removed thermally, which substantially increases energy use. A recent process model by Sánchez-Rivera et al. estimated that dryers in STRAPTM

consume $3.5\text{--}5.3 \times 10^6$ MJ per year, representing approximately 50–60% of total electricity use.¹¹ Electricity is both the most expensive and the most environmentally impactful utility in STRAPTM, thus understanding the solvent retention is significant for improving process efficiency and scalability.¹⁹

Solvent retention is likely influenced by several factors. Rapid phase separation can trap solvent molecules within polymer-rich aggregates, and incomplete crystallization may leave amorphous regions that hold solvent.^{20,21} High-molecular weight polymers from dense entanglement networks that restrict solvent diffusion, slowing desorption during filtration.^{22,23} Thermodynamic interactions can further stabilize solvent molecules in the polymer matrix.^{24–26} Those aforementioned factors occur simultaneously, and we expect that solvent retention is determined by multiple factors, not a single dominant factor.

The objective of this work is to develop a fundamental understanding of solvent retention in polymer-solvent gels formed during STRAPTM and to identify the key factors that influence the amount of solvent entrapped during precipitation and filtration. We measured solvent retention for six polymers and nine solvents. A support vector regression (SVR) model was developed to predict the solvent retention and determine the feature contributions. The six features were used in the model (solvent vapor pressure, total Hansen solubility parameter, polymer molecular weight, Flory-Huggins interaction parameters, predicted solubility, and polymer-to solvent mass ratio). The combined experimental and modeling approach provides a predictive framework and mechanistic insight that can guide solvent selection and overall operation in STRAPTM.

2. Background

Solvent-based plastic recycling relies on differences in polymer-solvent interactions to selectively dissolve, separate, and recover specific polymer from mixed and multilayer feedstocks. Understanding the thermodynamic and structural factors that govern polymer dissolution and precipitation is therefore essential from interpreting solvent retention in polymer-solvent system. This section summarizes key concepts related to polymer-solvent interactions, precipitation mechanisms, gel formation, and diffusion constraints relevant to STRAP™.

2.1 Polymer-solvent thermodynamics

Polymer dissolution is governed by the solvent quality and the entropy loss associated with mixing large macromolecules.²⁷ Classical approaches such as Hansen solubility parameters and the Flory-Huggins interaction parameter are commonly used to estimate polymer-solvent affinity.²⁸ The Hansen solubility parameters decomposes cohesive energy into dispersion, polar, and hydrogen-bonding.²⁹ When the Hansen solubility parameter of solvent is sufficiently close to that of the polymer, dissolution is favored.

The Flory-Huggins parameter also provides a measure of polymer-solvent compatibility. A low Flory-Huggins parameter indicate favorable interactions, while high Flory-Huggins parameters correspond to poor solvent quality. However, the Flory-Huggins is sensitive to temperature, composition, and estimation method, and thus potentially introduces uncertainty.^{30,31} Predicted solubilities from conductor-like screening model for real solvent offer an alternative approach by capturing molecular surface charge distributions and calculating temperature-dependent solubility for

polymers in different solvent.³² It has been used to guide STRAPTM solvent selection and to design sequential dissolution schemes that target specific polymers.

2.2 Polymer precipitation and gel formation

During STRAPTM, once the dissolved polymer solution is cooled or an antisolvent is added, the system undergoes phase separation. Polymer-rich domains nucleate and grow, forming aggregates that ultimately connect into a three-dimensional network.³³ This network, combined with the entrapped solvent phase, forms what is referred to as a polymer-solvent gel in this study.²⁶

The structure of the gel can be different depending on polymer concentration, solvent quality, precipitation rate, and polymer molecular weight. Rapid precipitation can trap solvent within polymer-rich aggregates before chains have sufficient time to reorganize.^{20,21} Crystalline regions that form during precipitation typically exclude solvent as polymer chains pack into ordered structures.³⁴ In contrast, amorphous regions can retain significant amounts of solvent because they remain disordered and provide free volume for solvent molecules.

Polymer molecular weight is another important factor. High molecular weight polymers can restrict chain mobility and slow solvent redistribution during precipitation.²² Also, the high molecular weight polymers are more likely to have higher degree of entanglements, hindering solvent diffusion and leading to a greater solvent retention.²³

2.3 Diffusion in polymer-solvent gels

After precipitation, mechanical vacuum filtration is used to remove the freely draining solvent from the polymer-solvent gel. The remaining solvent is held either within amorphous regions, inside polymer-rich aggregates, or in nanoscale domains trapped by chain entanglement. Solvent diffusion from these domains requires molecular diffusion through the polymer matrix.

Diffusion in polymers is controlled by segmental mobility, temperature, solvent-polymer affinity. High molecular weight polymers exhibit reduced mobility, and strong polymer-solvent affinity also hinders solvent mobility and retained solvents in the matrix.³⁵ As a result, even after extended filtration, a significant amount of solvent remains entrapped and must be removed by thermal drying.

2.4 Motivation for this work

Although polymer-solvent interactions, precipitation mechanisms, and polymer diffusion behavior have been studied independently, there is limited understanding of how these factors combine to influence solvent retention in STRAPTM polymer-solvent gels. Multiple effects occur simultaneously and a quantitative framework that captures these relationships would support solvent selection and overall STRAPTM process.

3. Experimental methods

3.1 Materials

Polymers used in this study is polypropylene (PP), low-density polyethylene (LDPE, EG412, Westlake), high-density polyethylene (HDPE, Marlex HHM5502BN, Chevron Phillips), polyethylene terephthalates (PET, ES306030, GoodFellow), and polystyrene (PS, 182427, Sigma-Aldrich). Three PP with different molecular weights were used, denoted as PP-L (low molecular weight), PP-M (medium molecular weight), and PP-H (high molecular weight). Solvents were selected based on solubility predictions and prior use in STRAPTM processes. The solvents used were dodecane (Thermo Scientific Chemicals), n-decane ($\geq 95\%$, Sigma-Aldrich), 1-decanol ($\geq 98\%$, Sigma-Aldrich), dimethyl sulfoxide (DMSO, ACS reagent grade, Sigma-Aldrich), γ -valerolactone (GVL, ReagentPlus, Sigma-Aldrich), 1,2,4-trichlorobenzene (TCB, ReagentPlus, Sigma-Aldrich), aniline (ACS reagent grade, Sigma-Aldrich), and xylene (VWR Chemicals). All solvents were used as received without further purification.

3.2 STRAPTM Experimental Procedure

Figure 1 describes the experimental procedure. Polymer dissolution as performed by placing 0.5–5 g of resin and 50 g of solvent in a 250 ml round-bottom flask equipped with a reflux condenser connected to a cold-water line. The flask was partially immersed in a silicone oil bath and heated until a homogenous solution formed. Dissolution temperature were chosen based on computational solubility prediction and previously reported STRAPTM operating conditions.

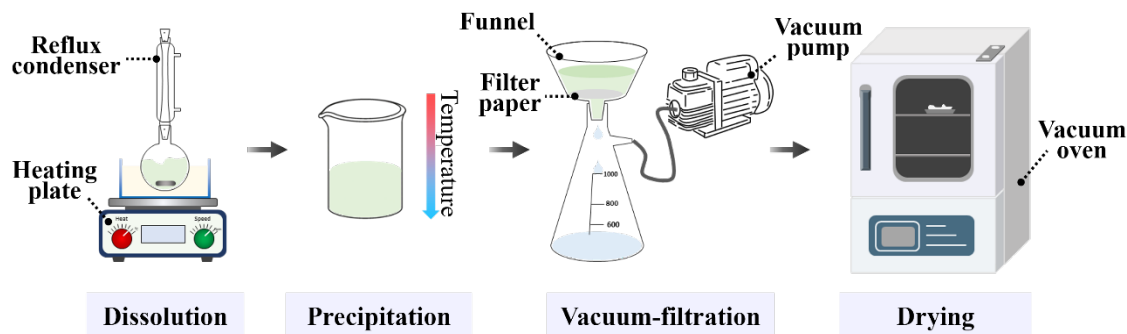


Figure 1. Experimental procedure for STRAP™. Polymer is dissolved in hot solvent, precipitated by cooling, vacuum-filtered, and finally dried in an oven to remove residual solvent.

After dissolution, the hot polymer solution was cooled or precipitated directly depending on the experimental condition. The resulting precipitated solution was vacuum filtered through 10 μm filter paper for 20 minutes to form a polymer-solvent gel. The mass of the wet gel (m_{gel}) was recorded immediately to form a polymer-solvent gel. The gel was subsequently dried in a vacuum oven at 100–130 $^{\circ}\text{C}$ for 2 hours, and the mass of the dried resin (m_{resin}) was measured. Thermogravimetric analysis (TGA) confirmed that no residual solvent remained after drying.

Solvent retention was calculated as the mass percentage of solvent held within the polymer-solvent gel after filtration according to Equation 1.

$$\text{Solvent retention (\%)} = \frac{m_{\text{gel}} - m_{\text{resin}}}{m_{\text{gel}}} \times 100 \quad (\text{Equation 1})$$

This procedure was repeated for selected polymer-solvent to evaluate reproducibility.

3.3 Cooling rate-controlled precipitation

A jacketed vessel connected to a chiller was built to control precipitation temperature as shown in Figure 2. Water from the chiller circulated through the jacket and maintained a constant vessel temperature. 2 g of LDPE dissolved in 150 g of xylene was transferred into the vessel. A temperature probe placed at the center of the solution recorded the temperature over time.

Cooling rate were determined by linearly fitting the temperature decrease during the first 100 seconds. Experiments were performed at vessel temperatures of 35, 60, and 80 °C. The resulting polymer-solvent gels after filtration were vacuum filtered and dried following the same procedure described above.

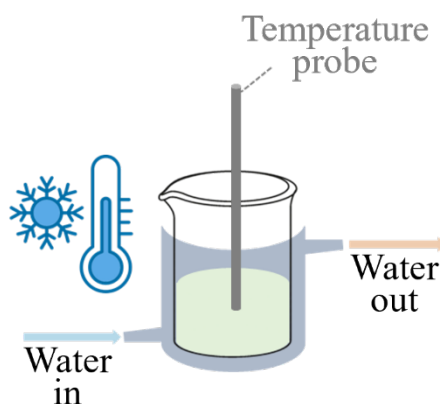


Figure 2. Schematic illustration of a jacketed vessel with two necks connected to a chiller.

3.4 Wide-Angle X-ray Scattering (WAXS)

Crystallinity measurements were performed on dried polymer samples obtained after precipitation and filtration. Samples were placed in a powder holder containing 15 circular holes with 2.5 mm diameter and were sealed with 12.5 μm Kapton tapes. WAXS

measurements were performed under vacuum at room temperature using Xeuss 3.0 system with an exposure time of 60 s.

Scattering patterns were corrected by subtracting Kapton background scattering using XSACT PRO software. Crystallinity (%) was determined by calculating the ratio of crystalline peak area to total scattering area after peak fitting.

3.5 Differential Scanning Calorimetry (DSC)

Melting temperature (T_m) and crystallization temperature (T_c) were measured using a DSC Q100 (TA Instruments). Samples were sealed in standard aluminum pans and heated or cooled at $10\text{ }^\circ\text{C min}^{-1}$ from 60 to $180\text{ }^\circ\text{C}$. The second heating cycle was used to determine T_m and T_c to eliminate prior thermal history.

3.6 Determination of variables

Six variables were selected as features to quantify their contributions to solvent retention. These variables represent solvent volatility, polymer-solvent affinity, and the initial composition of the dissolution mixture. Each variable was determined directly from experimental conditions or from established thermodynamic models used in prior STRAPTM studies.^{2,9-11,13,14}

Polymer molecular weights (M_w) were obtained either from the datasheets provided by manufacturer or from gel permeation chromatography (GPC) measurements performed. M_w strongly influences chain entanglement and diffusion, and M_w was included to account for polymer mobility in the polymer-solvent gel.

Solvent vapor pressure (P_{vap}) values at 25 °C were taken from the NIST Chemistry WebBook.³ P_{vap} was included to represent solvent volatility, which may influence solvent evaporation over the whole processes.

Hansen solubility parameters (δ_D , δ_P , δ_H) for each solvent were obtained from a published reference handbook.²⁹ The total Hansen solubility parameter (δ_T) was calculated from the three components using Equation 2.

$$\delta_T = \sqrt{\delta_D^2 + \delta_P^2 + \delta_H^2} \quad (\text{Equation 2})$$

δ_T reflects the combined dispersion, polar, and hydrogen-bonding interactions of solvent.

Flory-Huggins interaction parameters (χ) were calculated in the Equation 3 where V is the molar volume of the solvent, T is the absolute temperature, and R is the gas constant.³⁶

$$\chi = \frac{V (\delta_{\text{polymer}} - \delta_T)^2}{RT} \quad (\text{Equation 3})$$

Although χ is sensitive to temperature and estimation method, it was included as an initial variable to evaluate its predictive values.^{30,31}

Polymer-to-solvent mass ratio (r) was directly determined from the initial experimental condition by Equation 4.

$$r = \frac{m_{\text{polymer},0}}{m_{\text{solvent},0}} \quad (\text{Equation 4})$$

r describes the polymer concentration and viscosity, which indirectly influence solvent retention in the resulting gel.

Predicted solubility (S_{pred}) for PP, LDPE, HDPE, PET, PC, and PS was obtained using COSMO-RS calculations from our prior work.^{17,18} Polymer solubility in each solvent at the dissolution temperature was estimated using molecular models constructed from oligomer structures with deactivated terminal groups. These models were parameterized by reference melting temperatures and experimental solubilities, following established procedures from previous STRAPTM studies.^{9,11,17,18} COSMO-RS calculations were performed in COSMOtherm 19 using the BP_TZVP_19 parameterization, and solubilities were reported at the dissolution temperature used in each experiment.

3.7 SVR model

An SVR model was developed to predict the solvent retention and determine the variable contribution. All modeling was performed in Python using the scikit-learn library.³⁷

The initial model (Model 1) used all six variables (M_w , P_{vap} , δ_T , χ , S_{pred} , r). A five-feature model (Model 2) excluding χ and a four-feature model (Model 3) excluding both χ and r were also constructed to evaluate redundant or noisy variables.

Given the relatively small dataset ($n=34$), four-fold cross-validation was used.³⁸ Stratified sampling was performed by binning data at a solvent retention threshold of 60% to avoid bias toward high-retention samples.³⁹ This ensured that each fold contained a comparable distribution of both low and high retention samples.

Hyperparameters (C , ϵ , γ) were tuned through grid sweeping. The final parameters were presented in the table 1. These hyperparameters provided the best balance between bias and variance for each model.

Table 1. Hyperparameters of Model 1, 2, and 3.

| | C | ε | γ |
|---------|-----|---------------|----------|
| Model 1 | 70 | 0.05 | 0.3 |
| Model 2 | 80 | 0.01 | 0.55 |
| Model 3 | 100 | 0.01 | 0.55 |

Model performance was evaluated using the coefficient of determination (R^2), mean absolute error (MAE), and root-mean-square error (RMSE). The five-feature model produced the highest predictive accuracy ($R^2=0.78$) after removing χ .

Feature contributions were quantified using leave-one-feature-out (LOFO) analysis.⁴⁰ In LOFO, a model retrained after excluding one feature and the corresponding change in R^2 is computed. A large decrease in R^2 indicates a more important variable.

3.8 Model selection

Model selection was performed using the Akaike Information Criterion (AIC) and Bayesian Information Criterion (BIC) as shown in Equation 5 and 6.⁴¹

$$\text{AIC} = n \ln(\text{MSE}) + 2k \quad (\text{Equation 5})$$

$$\text{BIC} = k \ln(\text{MSE}) + k \ln(n) \quad (\text{Equation 6})$$

where n is the sample size, k represents model complexity, and MSE is the mean squared error. AIC applies a constant penalty on complexity ($2k$), while BIC imposes penalty which grows with sample size favoring simplicity more strongly, $k \ln(n)$.

The mean squared error was calculated using Equation 3.⁴² The squared residuals for each data point were summed and divided by the number of samples, assuming independent and normally distributed errors with zero mean and constant variance.

$$\text{MSE} = \frac{1}{n} \sum_i (y_i - \hat{y}_i)^2 \quad (\text{Equation 7})$$

where y_i and \hat{y}_i represent observed and predicted solvent retention values for sample, i , respectively.

4. Results and discussion

4.1 Conceptual overview of STRAP™

Figure 3 shows a conceptual schematic of how polymer-solvent gels form during the STRAP™ process. During dissolution, polymer chains disperse homogeneously in the solvent, forming a uniform polymer solution. When the solution is cooled, polymer-rich domains begin to nucleate and grow. Vacuum filtration separates the loose or residual solvent from the polymer-solvent gel. However, a fraction of solvent remains entrapped within the polymer-solvent gel. Rapid phase separation can trap solvent molecules inside polymer-rich aggregates before chains have time to reorganize.^{20,21} Amorphous regions do not fully expel solvent molecules, leaving a portion of the solvent in disordered matrix.³⁴ High molecular weight polymer forms dense entanglement networks that restrict chain mobility, slowing solvent diffusion. Strong polymer-solvent affinity limits the extent of solvent removal during vacuum filtration.³⁵ After filtration, the remaining solvent is removed by drying in the vacuum oven.

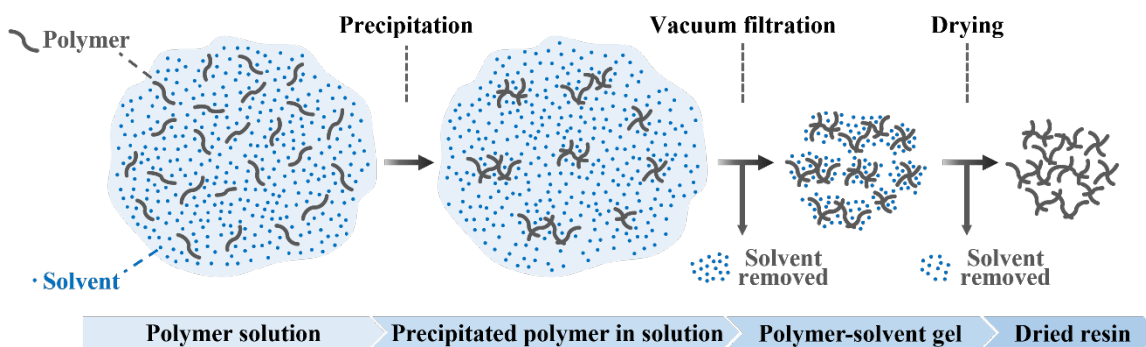


Figure 3. Conceptual schematic of polymer-solvent system during STRAP™. Blue dots and gray lines indicate solvent molecules and polymer chains.

4.2 Effect of cooling rate on crystallinity and solvent retention

A jacketed vessel was design for precise control of the cooling process as shown in Figure 2. The hot polymer solution was transferred to the jacketed vessel where the solution cooled isothermally at 35, 60, and 80 °C, and the temperature profile were recorded over time in Figure 4(a). The cooling rate were calculated as 0.047, 0.08, and 1.171 °C s⁻¹, respectively. Lower temperature resulted in faster cooling, and the solution temperature reached a steady state with the vessel after 2000 s.

WAXS measurements showed that LDPE crystallinity remained constant at 55%. Similarly, solvent retention values changed only slightly, ranging from 78 to 92% in Figure 4(b). These results indicate that the cooling rate has little influence on solvent retention in gels or crystallinity. Therefore, solvent retention in a polymer-solvent appears irrelevant to the cooling rate during precipitation.

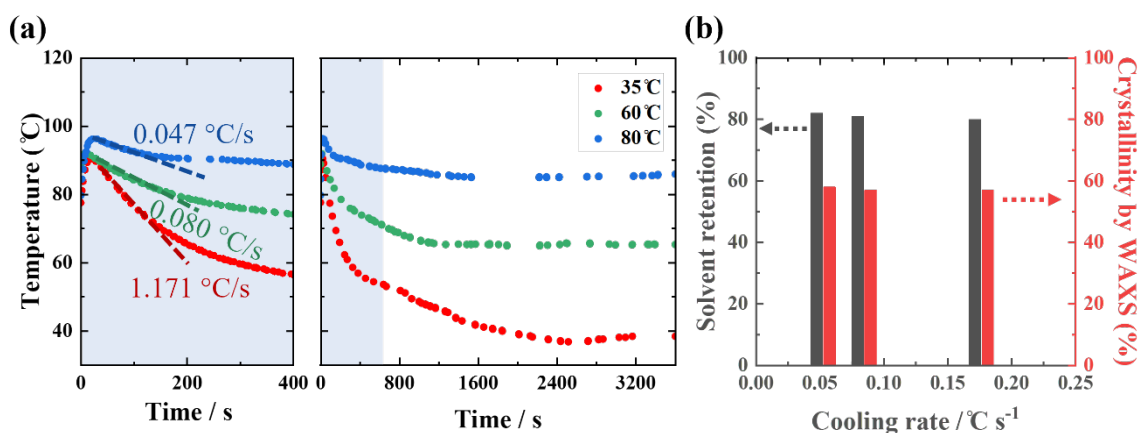


Figure 4. (a) Temperature profiles of hot polymer solution, cooled isothermally at different bath temperatures. The shaded region was used to determine the cooling rate. (b) Solvent retention and crystallinity as functions of the cooling rate.

4.3 Different precipitation methods

Two different precipitation was examined to determine whether it affects solvent retention in polymer-solvent gel. According to Sánchez-Rivera, precipitation can occur either by reducing the temperature or by adding an anti-solvent to induce phase separation.² Polymer solution were precipitated by adding 100 g of acetone and water as anti-solvents. Solvent retention of 78 and 79% were measured for acetone and water, respectively in Table 2. These values are comparable to ~80% obtained from temperature-controlled precipitation. These results demonstrate that the precipitation method has little impact on solvent retention in polymer-solvent gels.

Table 2. Solvent retention when anti-solvent is added.

| Anti-solvent | Solvent retention (%) |
|--------------|-----------------------|
| Acetone | 70 |
| Water | 100 |

4.4 Selective precipitation of PP and PE

Selective precipitation of PP and PE was then evaluated to determine whether temperature control could selectively induce crystallization of one polymer over the other.⁴³ Prior studies using temperature rising elution fractionation (TREF) and crystallization analysis fractionation (CRYSTAF) show evidence that differences in crystallization temperatures could allow PP to precipitate while PE remains dissolved.⁴⁴

Solution containing 2 g each of LDPE, PP-L, and PP-H in 150 g of xylene were precipitated at 50, 60, and 70 °C in Figure 5. Turbidity observations showed that lower temperatures resulted in greater turbidity due to reduced polymer solubility. Noticeably, LDPE solution remained clear at 70 °C, while both PP-L and PP-H appeared cloudy. This observation suggested the selective precipitation of PP from PE.

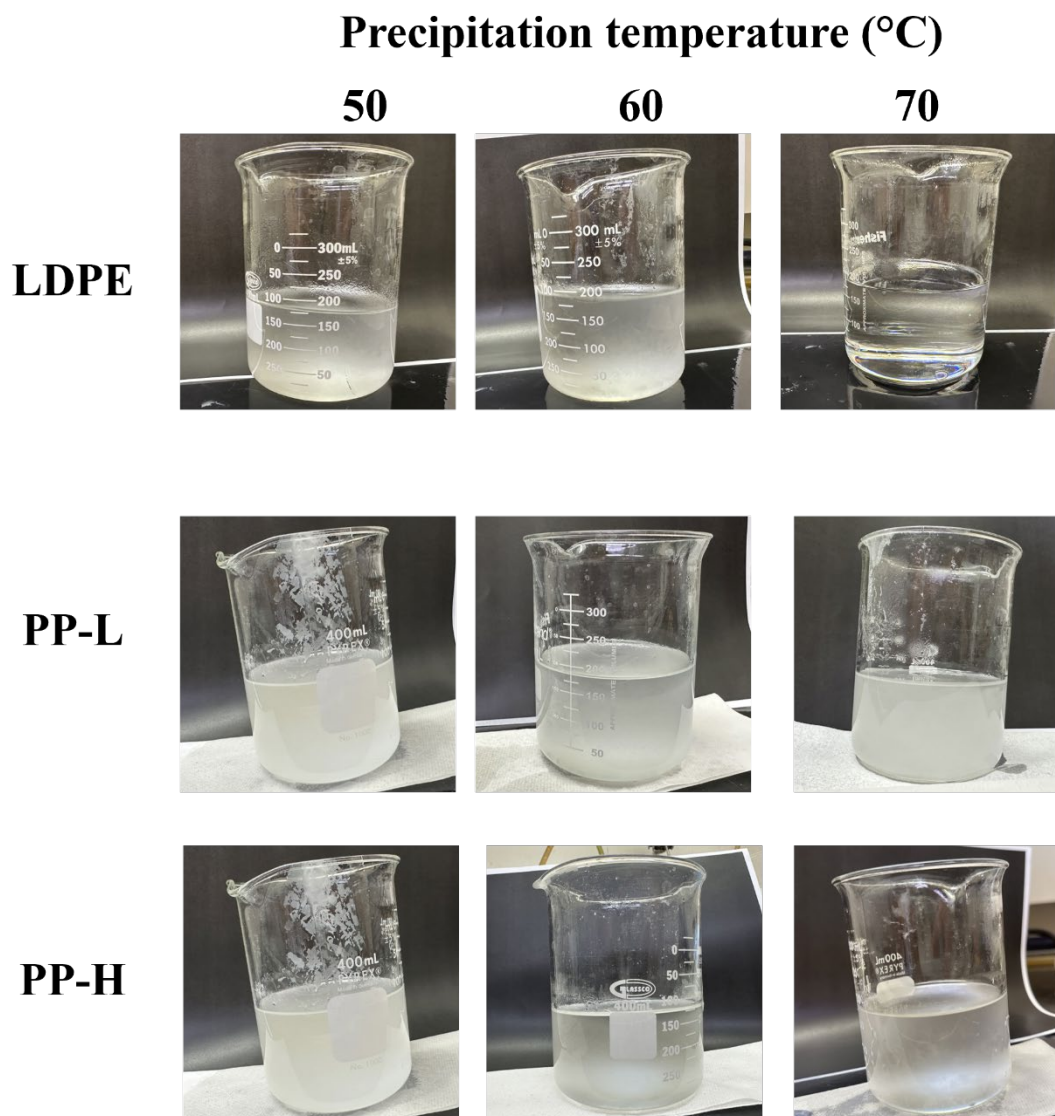


Figure 5. Images of 2 g of polymers (LDPE, PP-L, and PP-H) dissolved in 150 g of xylene precipitated at different temperatures in the jacketed vessel after 1 hr.

Equal masses (1 g each) of PP and LDPE were dissolved in xylene and precipitated at 70 °C in the jacketed vessel. DSC was run to measure T_m and T_c after vacuum filtration and drying. Two melting peaks are observed at 110 and 157 °C assigned for LDPE and PP, while the peaks at 100 and 115 °C are attributed to the crystallization of LDPE and PP in Figure 6.⁴⁵ The presence of both T_m and T_c for both LDPE and PP indicates that temperature-controlling precipitation does not allow selective precipitation of PP from LDPE. Precipitation conditions, including cooling rate and precipitation method, show no influence on solvent retention or selective recovery. Solvent retention remained nearly constant at ~80% regardless of all precipitation conditions for LDPE and xylene.

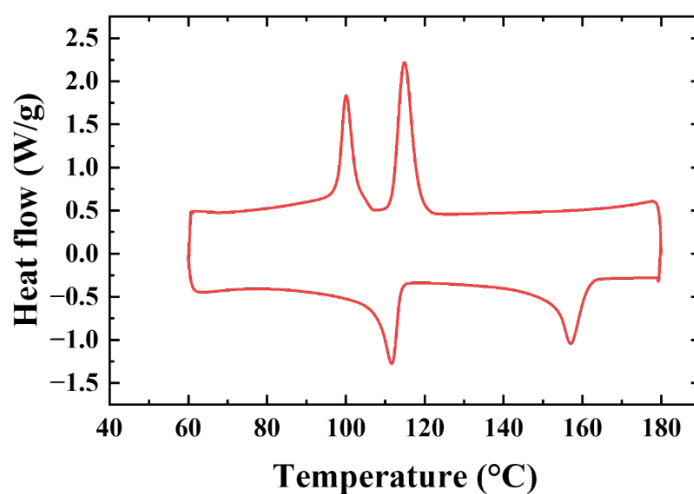


Figure 6. DSC curves (2nd heating cycling) for recovered PP and LDPE.

4.5 Effect of filtration time on solvent retention

Table 3 shows the effect of filtration time on solvent retention. The solvent retention is about 84% after 20 min of vacuum filtration and about 85% after 360 min of vacuum filtration for PP in decanol at a polymer-to-solvent ratio of 0.05. The negligible change in solvent retention with extended filtration time suggests that most of the freely draining solvent was removed within the first 20 min, and the remaining solvent is likely trapped within the polymer-solvent gel. Therefore, 20 min of vacuum filtration was considered sufficient and was used in all future experiments.

Table 3. Solvent retention of PP and decanol with 5 wt% with different filtration time.

| Polymers | Mw (g/mol) | Solvents | r | Filtration time (min) | Solvent retention (%) |
|----------|------------|----------|------|-----------------------|-----------------------|
| PP-L | 250,000 | Decanol | 0.05 | 20 | 83.75 |
| PP-L | 250,000 | Decanol | 0.05 | 360 | 85.22 |

4.6 Solvent retention in different polymer-solvent gels

Table 4 presents our experimental data from 34 experiments for measuring the solvent retention using six polymers and nine solvents. The polymers used in this work are PP, LDPE, HDPE, PET, PC, and PS. The solvents are xylene, decalin, aniline, TCB, dodecane, decane, decanol, GVL, and DMSO.

Table 4. Solvent retention in polymer-solvent gels with six variables including polymer-to-solvent ration (r), polymer molecular weights (M_w), solvent vapor pressure (P_{vap}), solvent Hansen solubility parameter (δ_T), predicted solubility (S_{pred}), and Flory-Huggins interaction parameter (χ).

| Experiment | Polymer | Solvent | r | M_w (g mol^{-1}) | P_{vap} (Pa, 25°C) | δ_T ($\text{MPa}^{0.5}$) | S_{pred} (wt %) | χ | Solvent retention (%) |
|------------|---------|----------|------|----------------------------------|--------------------------------|--------------------------------------|-----------------------------|--------|--------------------------|
| 1 | PP-L | Xylene | 0.01 | 250000 | 879 | 18.1 | 25.93 | 0.0005 | 20.16 |
| 2 | PP-L | Xylene | 0.05 | 250000 | 879 | 18.1 | 25.93 | 0.0005 | 36.69 |
| 3 | PP-L | Xylene | 0.05 | 250000 | 879 | 18.1 | 25.93 | 0.0005 | 40.37 |
| 4 | PP-L | Xylene | 0.05 | 250000 | 879 | 18.1 | 25.93 | 0.0005 | 39.44 |
| 5 | PP-M | Xylene | 0.05 | 423000 | 879 | 18.1 | 2.40 | 0.0005 | 59.85 |
| 6 | PP-H | Xylene | 0.05 | 821000 | 879 | 18.1 | 10.89 | 0.0005 | 52.30 |
| 7 | PP-L | Xylene | 0.1 | 250000 | 879 | 18.1 | 25.93 | 0.0005 | 47.98 |
| 8 | PP-L | Dodecane | 0.05 | 250000 | 18 | 16 | 23.40 | 0.3690 | 48.61 |
| 9 | PP-L | Dodecane | 0.05 | 250000 | 18 | 16 | 23.40 | 0.3690 | 52.53 |
| 10 | PP-M | Dodecane | 0.05 | 423000 | 18 | 16 | 8.26 | 0.3690 | 62.52 |

| | | | | | | | | | |
|----|------|----------|------|--------|-------|------|-------|--------|-------|
| 11 | PP-H | Dodecane | 0.05 | 821000 | 18 | 16 | 18.84 | 0.3690 | 79.51 |
| 12 | PP-L | Decane | 0.05 | 250000 | 190 | 15.7 | 27.67 | 0.4181 | 49.21 |
| 13 | PP-L | Decane | 0.05 | 250000 | 190 | 15.7 | 27.67 | 0.4181 | 55.34 |
| 14 | PP-L | Decanol | 0.05 | 250000 | 1.13 | 19.4 | 11.89 | 0.1517 | 83.75 |
| 15 | PP-L | Decanol | 0.05 | 250000 | 1.13 | 19.4 | 11.89 | 0.1517 | 79.47 |
| 16 | PP-L | Decalin | 0.05 | 250000 | 104.8 | 18 | 8.84 | 0 | 82.31 |
| 17 | PP-L | TCB | 0.05 | 250000 | 61.33 | 21.3 | 23.97 | 0.5513 | 85.60 |
| 18 | LDPE | Xylene | 0.05 | 86500 | 879 | 18.1 | 39.51 | 0.2194 | 35.56 |
| 19 | LDPE | Xylene | 0.05 | 86500 | 879 | 18.1 | 39.51 | 0.2194 | 36.94 |
| 20 | LDPE | Xylene | 0.05 | 86500 | 879 | 18.1 | 39.51 | 0.2194 | 39.45 |
| 21 | LDPE | Dodecane | 0.05 | 86500 | 18 | 16 | 57.46 | 0 | 73.07 |
| 22 | LDPE | Decane | 0.05 | 86500 | 190 | 15.7 | 61.67 | 0.0071 | 78.27 |
| 23 | LDPE | Decane | 0.05 | 86500 | 190 | 15.7 | 61.67 | 0.0071 | 75.44 |
| 24 | LDPE | Decanol | 0.05 | 86500 | 1.13 | 19.4 | 46.88 | 0.8945 | 67.18 |

| | | | | | | | | | |
|----|------|----------|------|--------|-------|------|-------|--------|-------|
| 25 | HDPE | Xylene | 0.05 | 143800 | 879 | 18.1 | 18.97 | 0.2194 | 30.32 |
| 26 | HDPE | Dodecane | 0.05 | 143800 | 18 | 16 | 39.79 | 0 | 85.79 |
| 27 | HDPE | Decane | 0.05 | 143800 | 190 | 15.7 | 44.00 | 0.0071 | 82.43 |
| 28 | HDPE | Decane | 0.05 | 143800 | 190 | 15.7 | 44.00 | 0.0071 | 85.45 |
| 29 | HDPE | Decanol | 0.05 | 143800 | 1.13 | 19.4 | 29.25 | 0.8945 | 86.35 |
| 30 | PET | DMSO | 0.05 | 35000 | 79.99 | 26.7 | 30.41 | 0.6354 | 92.33 |
| 31 | PET | Aniline | 0.05 | 35000 | 88.92 | 22.5 | 25.06 | 0.0092 | 89.38 |
| 32 | PET | GVL | 0.05 | 35000 | 31.33 | 23.2 | 40.11 | 0.0604 | 91.65 |
| 33 | PC | DMSO | 0.05 | 49218 | 79.99 | 26.7 | 17.24 | 1.4500 | 84.30 |
| 34 | PS | DMSO | 0.05 | 280000 | 79.99 | 26.7 | 22.47 | 1.8872 | 73.98 |

Figure 7 shows a box and scatter plot of the dataset presented in Table 4. Solvent retention spans 20.16 to 91.65% with first quartile (Q1) at 49.21% and the third quartile (Q3) at 84.3%. The median solvent retention, 73.98%, is greater than the mean, 67.16%, indicating the data is slightly concentrated at higher solvent retention. Solvent retention below Q1 was observed when xylene is used as solvent. This is because xylene has the highest vapor pressure, ~ 879 Pa.

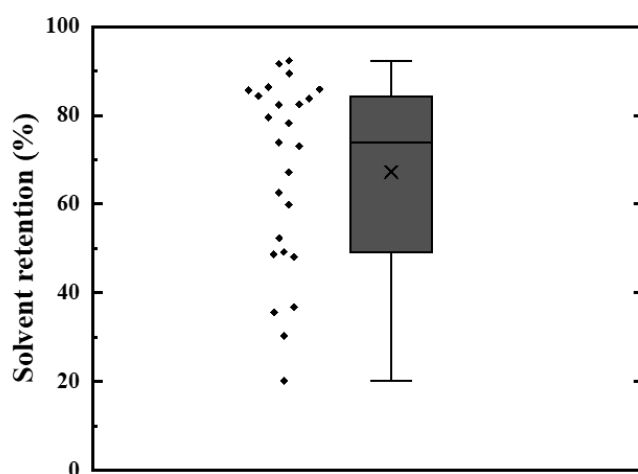


Figure 7. Box and scatter plot of measured solvent retention. The box shows the interquartile range with the median line. The “x” marks the average and two whiskers span the minimum and maximum values.

We correlated six variables with solvent retention. The six variables are P_{vap} , δ_T , χ , S_{pred} , r and M_w . P_{vap} describes solvent volatility of solvent while δ_T represents the combined contribution of dispersion, polar, and hydrogen-bonding interactions of solvents.²⁹ The polymer-solvent affinity is included using χ and S_{pred} from thermodynamic models, and r indicates the initial concentration and viscosity of the polymer solution. M_w determines the chain length and segmental mobility, which can

influence solvent retention through chain entanglements and restrict solvent diffusion in a polymer-solvent gel.

Spearman's rank correlation coefficients between solvent retention and each variable as shown in Figure 8. All absolute correlation were below 0.7, indicating that no single variable governs the solvent retention and instead it is an interplay from multiple variables. Although the correlations were generally low, P_{vap} and Mw exhibited relatively stronger correlation than other variables, suggesting that solvent volatility and polymer chain length are more closely related to solvent retention than other variables.

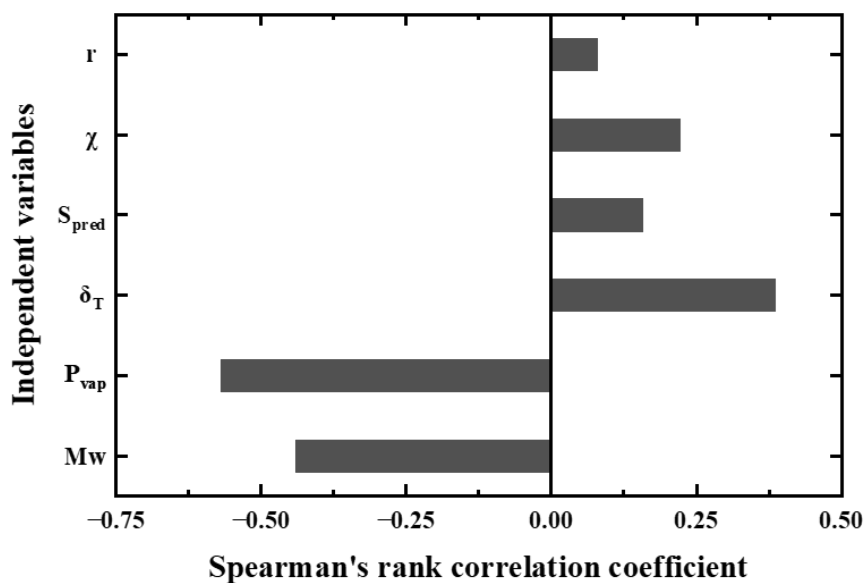


Figure 8. Spearman's rank correlation coefficient between each variable and solvent retention.

4.7 SVR model and model selection

To identify an appropriate regression model for solvent retention, we evaluated six supervised learning algorithms—SVR (RBF kernel), Ridge, ElasticNet, Random Forest, Gradient Boosting, and k-nearest neighbors (KNN) —across three feature sets in collaboration with Ali Altamimi as shown in Figure 9. Test R^2 values ranged from 0.56 to 0.78. The nonlinear methods (KNN and SVR) consistently achieved the highest performance, with SVR reaching a test R^2 of 0.78 for the five-feature and KNN yielding R^2 of 0.74 indicating that models designed for nonlinear relationships perform best. Tree-based methods (Random Forest and Gradient Boosting) showed intermediate performance, while linear models (Ridge and ElasticNet) performed worse overall. Due to the limited number of datasets and non-linear behavior, we selected SVR as the primary model for analyzing the solvent retention. All models were trained and assessed using stratified cross-validation, with solvent retention binned at a 60% threshold to maintain balanced representation of low- and high-retention samples in each split.

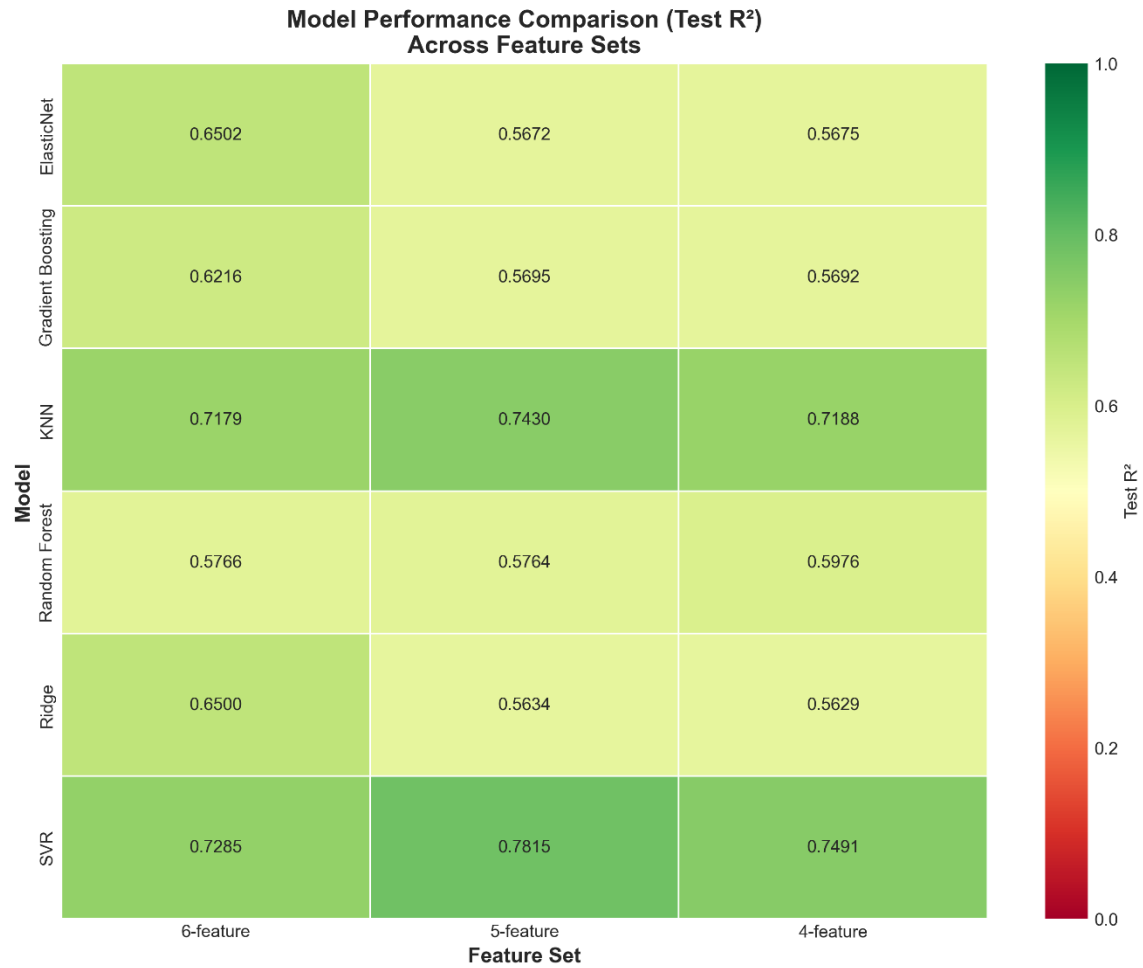


Figure 9. Tested R² of different models with six, five, and four features.

Feature selection was evaluated using a leave-one-out approach where each variable was dropped at a time and the cross-validated R^2 was recalculated, shown in Figure 10 and 11. The six-feature model achieved R^2 of 0.74, MAE of 8.84, and RMSE of 10.74 while the five-feature model removing χ exhibited R^2 of 0.78, MAE of 8.26, and RMSE of 8.77 showing slightly improvement in performance. Noticeably, the four-feature model without χ and r shows performance drop ($R^2=0.75$, MSE=9.9, and RMSE=10.3).

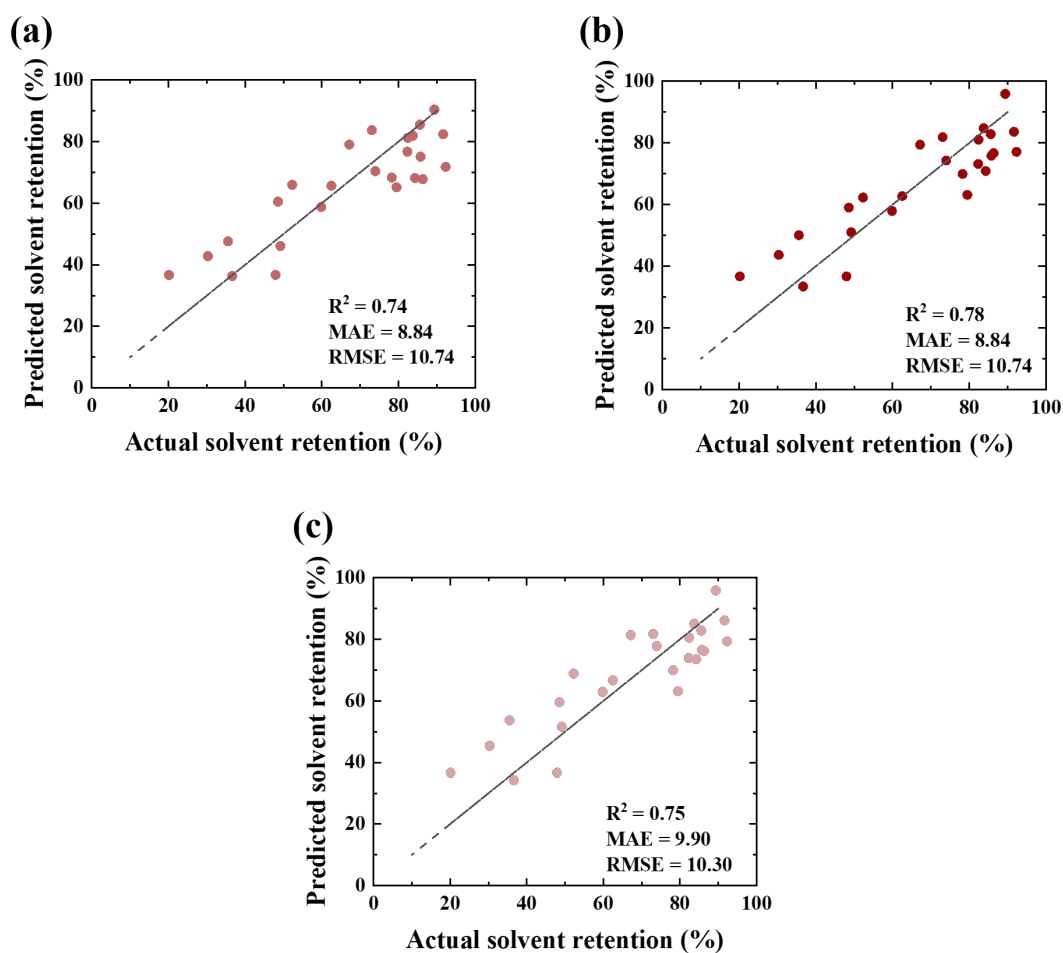


Figure 10. Parity plot of (a) six-, (b) five-, and (c) four-feature models.

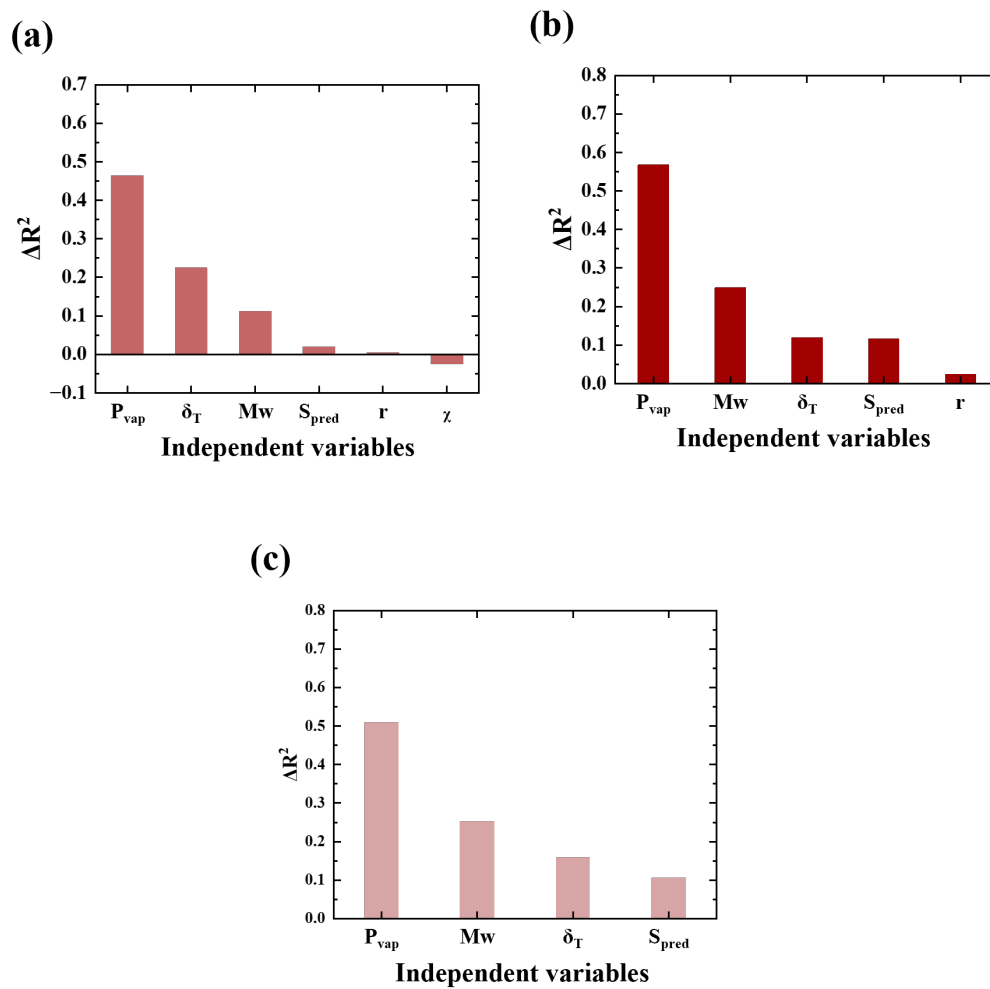


Figure 11. Leave-one-out analysis for (a) six-, (b) five-, and (c) four-feature models.

Table 5 summarizes the AIC and BIC used to assess the tradeoff between model fit and complexity for the six-, five-, and four-feature SVR models. Both criteria decrease moderately for the five-feature model relative to the six-feature model, showing $\Delta\text{AIC} = -4.7$, and $\Delta\text{BIC} = -4.7$. This suggests that removing χ improves overall predictive performance. In contrast, four-feature model shows a slight increase in AIC and BIC compared with the five-feature model, indicating the five-feature model is the ideal for predicting solvent retention.

Table 5. Models with six, five, and four features and their fitness and complexity.

| Features | DOF | R ² | AIC | BIC |
|---|-----|----------------|--------|---------|
| P _{vap} , δ_T , Mw, S _{pred} , r, and χ | 6 | 0.74 | 176.70 | 212.05 |
| P _{vap} , δ_T , Mw, S _{pred} , and r | 5 | 0.78 | 171.98 | 207.311 |
| P _{vap} , δ_T , Mw, and S _{pred} | 4 | 0.75 | 174.56 | 209.91 |

P_{vap} is the strongest variable to predict the solvent retention in the six-, five-, and four-feature models. It is followed by Mw, δ_T , S_{pred}, and r in the five-feature model.

5. Conclusions

This study provides a fundamental understanding of solvent retention in polymer-solvent gels formed during STRAPTM. We identified the key factors that play the dominant roles in determining solvent retention by combining experimental measurements with data-driven modeling.

Precipitation conditions and methods, including cooling rate and the use of anti-solvents, were found to have minimal influence on both the crystallinity (~55 %) and solvent retention (~80 %) of LDPE-xylene gels. Similarly, extended filtration led to negligible changes in solvent retention, indicating that only free solvent is removed during filtration while the remaining solvent remains entrapped within polymer-solvent gel.

In this study we measured the solvent retention in 34 different polymer-solvent gels including eight different polymers and nine different solvents. The solvent retention ranged from 20.16 to 91.65 wt% with a median value of 67.16 wt%. We developed a five-feature model to predict the solvent retention using SVR. The most important variable was the vapor pressure of the solvent, followed by $\delta_T > S_{pred} > M_w > r$. The model achieved R^2 of 0.78, demonstrating strong predictive capability for solvent retention in polymer-solvent gel.

Overall, this study establishes a quantitative framework to describe and predict the solvent retention in STRAPTM. The results highlight that controlling solvent volatility is more critical than adjusting precipitation or filtration conditions for minimizing residual solvent in polymer-solvent gels.

6. Future work

This study focused on solvent retention in single polymer systems, but future work should extend this approach to mixed and multilayer plastic waste. Real waste streams contain combinations of PE, PP, PET, and various adhesive or coating, and applying the same analysis to the systems would provide a more complete understanding of solvent retention during STRAPTM.

Zheng et al. proposed an automated sequence for solvent selection in which target polymers can be selectively dissolved. Integrating the solvent retention model developed in this work with Dr. Zheng's framework would provide a more comprehensive screening tool. For example, if several candidate solvents satisfy criteria in Zheng's framework, the SVR model reported here could be used to choose solvents that also minimize solvent retention. It will help reduce energy in drying and make STRAPTM more energy-efficient.

In addition, studying kinetics of solvent removal and precipitation would be one potential direction. While this work focused on evaluating features influencing solvent retention, the rate at which precipitation occurs and the rate at which solvent diffuses out of polymer aggregates may also influence retention under certain conditions. Dissolution kinetics have been previously studied by De Meester's group, and precipitation can be considered the reverse process. Understanding the kinetics on both sides may reveal additional relationships that were not captured in this work.

To conclude, extending this work to multilayer waste, integrating the model with the automated sequences for solvent selections, and studying precipitation and solvent-removal kinetics could build a more complete foundation for STRAPTM process.

7. References

- (1) Xu, Z.; Sanchez-Rivera, K.; Granger, C.; Zhou, P.; Munguia-Lopez, A. del C.; Ikegwu, U. M.; Avraamidou, S.; Zavala, V. M.; Van Lehn, R. C.; Bar-Ziv, E.; De Meester, S.; Huber, G. W. Solvent-Based Plastic Recycling Technologies. *Nat Chem Eng* **2025**, *2* (7), 407–423. <https://doi.org/10.1038/s44286-025-00247-1>.
- (2) Sánchez-Rivera, K. L.; Zhou, P.; Kim, M. S.; González Chávez, L. D.; Grey, S.; Nelson, K.; Wang, S.-C.; Hermans, I.; Zavala, V. M.; Van Lehn, R. C.; Huber, G. W. Reducing Antisolvent Use in the STRAP Process by Enabling a Temperature-Controlled Polymer Dissolution and Precipitation for the Recycling of Multilayer Plastic Films. *ChemSusChem* **2021**, *14* (19), 4317–4329. <https://doi.org/10.1002/cssc.202101128>.
- (3) Informatics, N. O. of D. and. *NIST Chemistry WebBook*. <https://webbook.nist.gov/chemistry/> (accessed 2025-10-20).
- (4) Andrady, A. L.; Neal, M. A. Applications and Societal Benefits of Plastics. *Philosophical Transactions of the Royal Society B: Biological Sciences* **2009**, *364* (1526), 1977–1984. <https://doi.org/10.1098/rstb.2008.0304>.
- (5) Thompson, R. C.; Swan, S. H.; Moore, C. J.; vom Saal, F. S. Our Plastic Age. *Philosophical Transactions of the Royal Society B: Biological Sciences* **2009**, *364* (1526), 1973–1976. <https://doi.org/10.1098/rstb.2009.0054>.
- (6) Uekert, T.; Singh, A.; DesVeaux, J. S.; Ghosh, T.; Bhatt, A.; Yadav, G.; Afzal, S.; Walzberg, J.; Knauer, K. M.; Nicholson, S. R.; Beckham, G. T.; Carpenter, A. C. Technical, Economic, and Environmental Comparison of Closed-Loop Recycling Technologies for Common Plastics. *ACS Sustainable Chem. Eng.* **2023**, *11* (3), 965–978. <https://doi.org/10.1021/acssuschemeng.2c05497>.
- (7) Geyer, R.; Jambeck, J. R.; Law, K. L. Production, Use, and Fate of All Plastics Ever Made. *Science Advances* **2017**, *3* (7), e1700782. <https://doi.org/10.1126/sciadv.1700782>.
- (8) Schyns, Z. O. G.; Shaver, M. P. Mechanical Recycling of Packaging Plastics: A Review. *Macromolecular Rapid Communications* **2021**, *42* (3), 2000415. <https://doi.org/10.1002/marc.202000415>.
- (9) Walker, T. W.; Frelka, N.; Shen, Z.; Chew, A. K.; Banick, J.; Grey, S.; Kim, M. S.; Dumesic, J. A.; Van Lehn, R. C.; Huber, G. W. Recycling of Multilayer Plastic Packaging Materials by Solvent-Targeted Recovery and Precipitation. *Science Advances* **2020**, *6* (47), eaba7599. <https://doi.org/10.1126/sciadv.aba7599>.
- (10) Sánchez-Rivera, K. L.; Zhou, P.; Radkevich, E.; Sharma, A.; Bar-Ziv, E.; Van Lehn, R. C.; Huber, G. W. A Solvent-Targeted Recovery and Precipitation Scheme for the Recycling of up to Ten Polymers from Post-Industrial Mixed Plastic Waste. *Waste Management* **2025**, *194*, 290–297. <https://doi.org/10.1016/j.wasman.2025.01.022>.

- (11) Sánchez-Rivera, K. L.; Munguía-López, A. del C.; Zhou, P.; Cecon, V. S.; Yu, J.; Nelson, K.; Miller, D.; Grey, S.; Xu, Z.; Bar-Ziv, E.; Vorst, K. L.; Curtzwiler, G. W.; Van Lehn, R. C.; Zavala, V. M.; Huber, G. W. Recycling of a Post-Industrial Printed Multilayer Plastic Film Containing Polyurethane Inks by Solvent-Targeted Recovery and Precipitation. *Resources, Conservation and Recycling* **2023**, *197*, 107086. <https://doi.org/10.1016/j.resconrec.2023.107086>.
- (12) Yan, T.; Granger, C.; Sánchez-Rivera, K. L.; Zhou, P.; Grey, S.; Nelson, K.; Long, F.; Bar-Ziv, E.; Van Lehn, R. C.; Avraamidou, S.; Huber, G. W. Pigment Removal from Reverse-Printed Laminated Flexible Films by Solvent-Targeted Recovery and Precipitation. *Science Advances* **2025**, *11* (11), eadt5841. <https://doi.org/10.1126/sciadv.adt5841>.
- (13) Sánchez-Rivera, K. L.; Granger, C.; Appiah, H.; Nelson, K.; Grey, S.; Sun, D. J.; Estela-García, J. E.; Chen, E.; Xu, Z.; Osswald, T. A.; Turng, L.-S.; McDonald, A. G.; Van Lehn, R. C.; Bar-Ziv, E.; Huber, G. W. Cast Film Production with Polyethylene Recycled from a Post-Industrial Printed Multilayer Film by Solvent-Targeted Recovery and Precipitation. *ACS Materials Lett.* **2024**, *6* (9), 4042–4050. <https://doi.org/10.1021/acsmaterialslett.4c01048>.
- (14) Yu, J.; Carmen Munguía-López, A. del; S. Cecon, V.; L. Sánchez-Rivera, K.; Nelson, K.; Wu, J.; Kolapkar, S.; M. Zavala, V.; W. Curtzwiler, G.; L. Vorst, K.; Bar-Ziv, E.; W. Huber, G. High-Purity Polypropylene from Disposable Face Masks via Solvent-Targeted Recovery and Precipitation. *Green Chemistry* **2023**, *25* (12), 4723–4734. <https://doi.org/10.1039/D3GC00205E>.
- (15) Tushar; Granger, C.; Altamimi, A.; Cortes-Pena, Y.; Nelson, K.; Dong, X.; Britt, K.; Barrows, L.; Thurnheer, A.; Avraamidou, S.; Van Lehn, R. C.; Huber, G. W. Recycling of Single-Use Multilayer Plastics for Biomanufacturing with Solvent-Targeted Recovery and Precipitation. *ACS Sustainable Chem. Eng.* **2025**, *13* (40), 16930–16945. <https://doi.org/10.1021/acssuschemeng.5c06479>.
- (16) Denolf, R.; Doolaege, J. C.; Selmurzaeva, E.; Manhaeghe, D.; De Somer, T.; Haris, M.; Vermeeren, N.; Kol, R.; Hogie, J.; De Meester, S. Understanding the Dissolution Kinetics of a DINCH Plasticized PVC: Experimental Design and Applied Modeling. *ChemSusChem* **2025**, *18* (17), e202401756. <https://doi.org/10.1002/cssc.202401756>.
- (17) Zhou, P.; Sánchez-Rivera, K. L.; Huber, G. W.; Van Lehn, R. C. Computational Approach for Rapidly Predicting Temperature-Dependent Polymer Solubilities Using Molecular-Scale Models. *ChemSusChem* **2021**, *14* (19), 4307–4316. <https://doi.org/10.1002/cssc.202101137>.
- (18) Zhou, P.; Yu, J.; Sánchez-Rivera, K. L.; Huber, G. W.; Lehn, R. C. V. Large-Scale Computational Polymer Solubility Predictions and Applications to Dissolution-

Based Plastic Recycling. *Green Chem.* **2023**, *25* (11), 4402–4414.
<https://doi.org/10.1039/D3GC00404J>.

(19) Chang, H.; Zhao, Y.; Xu, A.; Damgaard, A.; Christensen, T. H. Mini-Review of Inventory Data for the Dewatering and Drying of Sewage Sludge. *Waste Manag Res* **2023**, *41* (6), 1081–1088. <https://doi.org/10.1177/0734242X221139170>.

(20) Barham, P. J.; Selwood, A. Removal of Solvent from Gels of Poly(Hydroxybutyrate) and Shaped Articles Formed Therefrom. US4360488A, November 23, 1982. <https://patents.google.com/patent/US4360488A/en> (accessed 2025-11-19).

(21) He, J.; Kong, X.; Wang, Y.; Delaney, M.; Kalyon, D. M.; Lee, S. S. Crystallization-Arrested Viscoelastic Phase Separation in Semiconducting Polymer Gels. *ACS Appl. Polym. Mater.* **2019**, *1* (3), 500–508. <https://doi.org/10.1021/acsapm.8b00195>.

(22) Nahali, N.; Rosa, A. Nanoprobe Diffusion in Entangled Polymer Solutions: Linear vs. Unconcatenated Ring Chains. *J. Chem. Phys.* **2018**, *148* (19), 194902. <https://doi.org/10.1063/1.5022446>.

(23) Pawlak, A.; Krajenta, J. Progress in Studies of Disentangled Polymers and Composites. *Journal of Composites Science* **2023**, *7* (12), 521. <https://doi.org/10.3390/jcs7120521>.

(24) Kong, B. S.; Kwon, Y. S.; Kim, D. Theoretical and Experimental Analysis of Polymer Molecular Weight and Temperature Effects on the Dissolution Process of Polystyrene in Ethylbenzene. *Polym J* **1997**, *29* (9), 722–732. <https://doi.org/10.1295/polymj.29.722>.

(25) Tanner, J. E. Diffusion in a Polymer Matrix. *Macromolecules* **1971**, *4* (6), 748–750. <https://doi.org/10.1021/ma60024a015>.

(26) Wang, H.; Men, Y.; Tashiro, K. Solvent-Induced Crystallization and Phase-Transition Phenomena in Syndiotactic Polystyrene and Its Relatives. *Front. Soft Matter* **2022**, *2*. <https://doi.org/10.3389/frsfm.2022.1041872>.

(27) Venkatram, S.; Kim, C.; Chandrasekaran, A.; Ramprasad, R. Critical Assessment of the Hildebrand and Hansen Solubility Parameters for Polymers. *J. Chem. Inf. Model.* **2019**, *59* (10), 4188–4194. <https://doi.org/10.1021/acs.jcim.9b00656>.

(28) Lindvig, T.; Michelsen, M. L.; Kontogeorgis, G. M. A Flory–Huggins Model Based on the Hansen Solubility Parameters. *Fluid Phase Equilibria* **2002**, *203* (1), 247–260. [https://doi.org/10.1016/S0378-3812\(02\)00184-X](https://doi.org/10.1016/S0378-3812(02)00184-X).

(29) Hansen, C. M. *Hansen Solubility Parameters: A User's Handbook*, 2nd ed.; CRC Press: Boca Raton, 2007.

(30) Clarke, C. J.; Eisenberg, A.; La Scala, J.; Rafailovich, M. H.; Sokolov, J.; Li, Z.; Qu, S.; Nguyen, D.; Schwarz, S. A.; Strzemechny, Y.; Sauer, B. B. Measurements of the

Flory–Huggins Interaction Parameter for Polystyrene–Poly(4-Vinylpyridine) Blends. *Macromolecules* **1997**, *30* (14), 4184–4188. <https://doi.org/10.1021/ma961135l>.

(31) Willis, J. D.; Beardsley, T. M.; Matsen, M. W. Simple and Accurate Calibration of the Flory–Huggins Interaction Parameter. *Macromolecules* **2020**, *53* (22), 9973–9982. <https://doi.org/10.1021/acs.macromol.0c02115>.

(32) Klamt, A. Conductor-like Screening Model for Real Solvents: A New Approach to the Quantitative Calculation of Solvation Phenomena. *J. Phys. Chem.* **1995**, *99* (7), 2224–2235. <https://doi.org/10.1021/j100007a062>.

(33) Zhu, P.; Cai, Z.; Shi, J.; Zhu, C.; Wang, M.; Wang, C.; Zhang, H. Liquid–Liquid Phase Separation, Crystallization, and Solvent Evaporation in Relation to Microsphere Formation from Isotactic Polypropylene Solution. *J. Phys. Chem. B* **2025**, *129* (25), 6320–6333. <https://doi.org/10.1021/acs.jpcc.5c00135>.

(34) Wang, H.; Men, Y.; Tashiro, K. Solvent-Induced Crystallization and Phase-Transition Phenomena in Syndiotactic Polystyrene and Its Relatives. *Front. Soft Matter* **2022**, *2*. <https://doi.org/10.3389/frsfm.2022.1041872>.

(35) Kozanecki, M.; Halagan, K.; Saramak, J.; Matyjaszewski, K. Diffusive Properties of Solvent Molecules in the Neighborhood of a Polymer Chain as Seen by Monte-Carlo Simulations. *Soft Matter* **2016**, *12* (25), 5519–5528. <https://doi.org/10.1039/C6SM00569A>.

(36) Danner, R. P.; High, M. S. *Handbook of Polymer Solution Thermodynamics*; John Wiley & Sons, 2010.

(37) SVR. scikit-learn. <https://scikit-learn/stable/modules/generated/sklearn.svm.SVR.html> (accessed 2025-10-20).

(38) 3.1. Cross-validation: evaluating estimator performance. scikit-learn. https://scikit-learn/stable/modules/cross_validation.html (accessed 2025-10-20).

(39) StratifiedShuffleSplit. scikit-learn. https://scikit-learn/stable/modules/generated/sklearn.model_selection.StratifiedShuffleSplit.html (accessed 2025-10-20).

(40) LeaveOneOut. scikit-learn. https://scikit-learn/stable/modules/generated/sklearn.model_selection.LeaveOneOut.html (accessed 2025-10-20).

(41) Chakrabarti, A.; Ghosh, J. K. AIC, BIC and Recent Advances in Model Selection. In *Philosophy of Statistics*; Bandyopadhyay, P. S., Forster, M. R., Eds.; Handbook of the Philosophy of Science; North-Holland: Amsterdam, 2011; Vol. 7, pp 583–605. <https://doi.org/10.1016/B978-0-444-51862-0.50018-6>.

(42) Wang, W.; J. Dziedzic, O.; R. Lesnjak, C.; Yu, Z.; Miller, J.; Shi, X.; R. Featherman, J.; A. Rankin, S.; W. Huber, G. The Kinetics of Aqueous Lactose

Hydrolysis with Sulfuric Acid. *Reaction Chemistry & Engineering* **2025**, *10* (7), 1676–1691. <https://doi.org/10.1039/D5RE00175G>.

(43) Cicolella, A.; De Stefano, F.; Scoti, M.; Talarico, G.; Eagan, J. M.; Coates, G. W.; Di Girolamo, R.; De Rosa, C. Phase Separation and Crystallization in Monodisperse Block Copolymers of Linear Low-Density Polyethylene and Isotactic Polypropylene. *Macromolecules* **2024**, *57* (5), 2230–2245. <https://doi.org/10.1021/acs.macromol.3c02470>.

(44) Monrabal, B.; del Hierro, P. Characterization of Polypropylene–Polyethylene Blends by Temperature Rising Elution and Crystallization Analysis Fractionation. *Anal Bioanal Chem* **2011**, *399* (4), 1557–1561. <https://doi.org/10.1007/s00216-010-4061-5>.

(45) Aumnate, C.; Rudolph, N.; Sarmadi, M. Recycling of Polypropylene/Polyethylene Blends: Effect of Chain Structure on the Crystallization Behaviors. *Polymers (Basel)* **2019**, *11* (9), 1456. <https://doi.org/10.3390/polym11091456>.